Indian Journal of Chemistry
Vol. 64, February 2025, pp. 232-246
DOI: 10.56042/ijc.v64i2.16198

Identification of dual human acetylcholinesterase and butyrylcholinesterase inhibitors through pharmacophore-based virtual screening, molecular docking and molecular dynamics simulation studies

Poonam Yadav & Shivani Jaiswal*

Institute of Pharmaceutical Research, GLA University, Mathura 281 406, India

E-mail: shivani.rs.phe16@iitbhu.ac.in, shivanijaiswal.2010@rediffmail.com

Received 4 January 2025; accepted (revised) 22 January 2025

The concomitant inactivation of both human acetylcholinesterase (hAChE) and butyrylcholinesterase (hBuChE) is a significant factor in the therapeutic approach to AD. The objective of this research is to use *in silico* methodologies namely, pharmacophore-based virtual screening and molecular docking to find potential dual inhibitors targeting both hAChE and hBuChE. Six features' pharmacophores have been developed using structure-based drug design for AChE and BuChE enzymes and the developed pharmacophores have been validated using the Gunery-Henery (GH) Scoring method. The GH scores have been found in the acceptable range; 0.779 for AChE and 0.833 for BuChE-based pharmacophore. Further validated pharmacophores have been used for exploring the ZINC database to retrieve the novel hits employing various parameters *viz* fit value, Lipinski rule of five violation, and feature mapping. After the virtual screening process, 11 molecules have been retrieved which are further subjected to molecular docking to determine the binding interactions with the AChE and BuChE enzymes' active binding sites using the LibDock module in DS 2.0 software. Based on binding energy and binding interactions, three molecules have been selected for the molecular dynamic (MD) simulation and *in silico* pharmacokinetics. Finally, MD simulation and *in silico* pharmacokinetics analysis have exhibited that **ZINC000329492445**, **ZINC000001693021**, and **ZINC000257331938** molecules can be potential dual inhibitors against hAChE and hBuChE.

Keywords: Alzheimer's disease, Structure-based drug design, Virtual screening, Molecular dynamic simulation, *In silico* pharmacokinetics

Alzheimer's disease (AD) is a neurological condition that is characterized by permanent cognitive decline and gradual memory loss, and is recognized as the primary cause of dementia among the aged population worldwide[1]. This ailment accounts for around 60% to 70% of instances of cognitive decline known as dementia, which now afflicts a global population exceeding 30 million individuals[2]. The exact cause of AD is still unknown, but research suggests that neuroinflammation (oxidative stress and reactive oxygen species), reduced acetylcholine (ACh) concentration, accumulation of amyloid-beta plaques, and aggregation of tau proteins in the brain are significant factors contributing to the progression of the disease[3]. According to diversified theory of AD, cognitive degradation is associated with the interruption of cholinergic pathways in the cerebral cortex and basal forebrain, as well as a drop in ACh levels[4]. According to Ferreira-Vieira *et al*. (2016), the cholinergic hypothesis seems to be the most plausible mechanism for elucidating the cognitive and behavioral alterations seen in older individuals, as well as serving as the primary focus for current pharmacological interventions for Alzheimer's disease[5]. Human cholinesterases, namely acetylcholinesterase (hAChE, E.C 3.1.1.7) and butyrylcholinesterase (hBuChE, E.C 3.1.1.8), are a group of enzymatic catalysts that are essential for the degradation of ACh. These enzymes exhibit variations in their tissue distribution. The enzyme acetylcholinesterase (AChE) is mostly present in the central nervous system (CNS) and serves as the primary catalyst for the hydrolysis of acetylcholine. Conversely, butyrylcholinesterase (BuChE) is primarily linked with glial cells and is predominantly detected in the plasma[6]. Experimental pieces of shreds demonstrated an elevation in hBuChE levels inside the memory-related regions of the brain, namely those related to learning and memory. This rise is coupled with the inhibition of hAChE and is believed to serve as a compensation mechanism for the loss in hAChE activity[7,8]. Dual inhibition of human cholinesterase using hAChE and hBuChE has shown clinical efficacy in the symptomatic management of AD. Moreover, the inhibition of hBuChE has been shown to be associated

with a decrease in the development of amyloid plaques[9].

Currently, Food and Drug Administration (FDA) has approved four anticholinesterase drugs for the treatment of AD donepezil, galantamine (inhibitors of human acetylcholinesterase), rivastigmine, and tacrine (inhibitors of both human acetylcholinesterase and human butyrylcholinesterase)[10]. These drugs have demonstrated intellectual, operational, and behavioral benefits in alleviating the manifestations of the disease. In spite of the positive outcomes seen in the symptomatic treatment of AD, there have been reports of significant side effects associated with currently existing pharmaceuticals and the design of AD medications[11]. These adverse effects include but are not limited to diarrhea, dizziness, cramping in the muscles, hypotension, insomnia, exhaustion, and diminished appetite. Therefore, it is essential to conduct a search for novel dual inhibitors targeting both hAChE and hBuChE enzymes, which possess favorable pharmacokinetic properties and low toxicity[12,13].

The possible approach for prioritizing dual inhibitors involves the identification of stereo-electronic characteristics in compounds exhibiting dual biological activity against hAChE and hBuChE. This strategy aids in the exploration of novel compounds possessing these specific attributes, such as using pharmacophore models. According to Zhou *et al*. (2019), the combination of pharmacophore models, molecular docking investigations, and pharmacokinetic prediction may be used to prioritize bioavailable molecules that exhibit the same binding mechanism as existing medications[14]. Therefore, the use of progressive simulated screening techniques, such as *in silico* based pharmacophore models and molecular docking, might prove to be advantageous in the identification of possible dual cholinesterase inhibitors that exhibit enhanced affinity[15,16].

The primary objective of present work is to construct a pharmacophore model for dual cholinesterase inhibitors and use computational methods to discover compounds with high affinity for both human acetylcholinesterase (hAChE) and human butyrylcholinesterase (hBuChE), with considering their bioavailability.

Material and methods

Preparation of data set

Prior to the computational analysis, the ligand structures were downloaded in sdf format from ZINC database under the label “all screening compounds” which include 125757 molecules[17]. The structures were screened for drug-likeness using the Lipinski rule of five[18].

Structure-based drug design (SBDD)

X-ray crystallography structure of AChE (4ey7) and BuChE (5dyw) were retrieved from the protein databank (PDB) https://www.rcsb.org[19,20]. Structure-based pharmacophore models were developed using the receptor-pharmacophore generation module of Accelrys Discovery Studio 2.0 (Ref. 18). The approach facilitates the generation of potential pharmacophores by extracting binding characteristics, namely intermolecular non-covalent interactions between receptors and ligands[21]. The six distinct pharmacophore types that are being used, namely: hydrophobic features, aromatic rings, hydrogen bond acceptors (HBA) and donors (HBD), and positive and negative ionizable centers (Pos_ionizable and Neg_ionizable, respectively)[22]. Prior to modeling, it has been verified that both the protein and ligands have entire valence shells. The methodology includes the excluded volumes with a radius of 9 Å to indicate the area that is inaccessible to the bound ligand inside the receptor binding site. Additionally, the Güner-Henry (GH) scoring system was used to assess the construction of the pharmacophore models' performance. The GH score was derived by calculating the following metrics. Let D represent the overall quantity of molecules included within the database. Similarly, a denotes the total count of active molecules existing in the database. Ht signifies the cumulative number of hits acquired *via* the implementation of a pharmacophore-based search inside the database. Ha, on the other hand, represents the true positives, namely the quantity of active molecules that are included within the produced hit list. The variable Y represents the recall, which is defined as the percentage of active molecules obtained from the database hits. Conversely, precision (represented by variable A) is the proportion of active molecules that were appropriately identified from the database search. Contrasting the GH score, the E value (enrichment factor) provides an estimate by measuring the number of active compounds obtained *via* a database search. The ideal model, which is seldom attained by random experimentation, has a GH score of 1, whereas a score between 0.7 and 0.8 indicates a very noteworthy model. The larger the E

number, the more efficient the model is in sifting through a chemical library in search of active molecules[23].

Virtual screening

Pharmacophore-based virtual screening is a powerful tool to identify structurally diverse and promising lead compounds from a broad chemical compound database[24]. The validated pharmacophore was employed to explore the Zinc database, containing 125757 compounds for the retrievation of the best-fit compounds. The retrieved compounds were checked for Lipinski's violation. Further, molecules were filtered according to their fit and estimated values to get the most potent set of molecules as AChE and BuChE inhibitors.

Molecular docking

The 3D structure of AChE and BuChE revealed that the active site of the AChE (PDB ID: 4ey7) and BuChE (PDB ID: 5dyw) possess a small rectangular cavity, pre-bonded with the standard molecule donepezil and N-((1-benzylpiperidin-3-yl) methyl)-N-(2-methoxyethyl) naphthalene-2-sulfonamide respectively to form a co-crystal. The active binding sites are of AChE comprises of Ser203, Phe295, Tyr72, Trp286, Tyr341, Tyr337, Phe338 and Trp86[25,26]; Whereas, BuChE active binding sites are comprises of Thr120, Asn68, Gly116, Leu286, Trp231, Phe329, Tyr332, Ala328, and Trp82 as important amino acid residues[27]. The LibDock protocol on Discovery Studio (DS) 2.0 was used to dock the filtered molecules in that active site. Protein preparation module was used for the preparation of the protein[28]. For the protein preparation, hydrogen atoms were added along with removing molecules of water with satisfying CHARMM force fields[29]. Using the co-crystallized ligand's geometric centroid, the active sites were defined as a sphere of 9Å. All retrieved molecules were used for docking into the active binding sites of the prepared protein. LibDock methods produced more than 100 different poses for each retrieved molecule. During docking, the best conformational approach was used, with each molecule having a maximum of 255 confirmations within a 20 kcal/mol energy range above the global energy lowest threshold. Ten hotspots were created for each docking[14]. The scoring function along with binding interactions for each conformational posture was used as selection criteria throughout the study. More desired hit molecules were those that showed interactions with required active site residues with a high docking score.

Molecular dynamic simulation (MDS)

In order to assess the credibility of the docking results, molecular dynamics simulations (MDS) were conducted with the Desmond software (Schrodinger Release 2020-3)[30,31]. All systems were prepared by the system builder tool. The solvent model with an orthorhombic box was selected as TIP3P (transferable intermolecular interaction potential 3 points). The OPLS_2005 force field was used in the simulation. The models were made neutral by adding counter ions where needed. To mimic the physiological conditions, 0.15 M salt (NaCl) was added. The NPT ensemble with 300 K temperature and 1 atm pressure was selected for complete simulation. The protein structures, namely 4ey7 and 5dyw, together with their respective complexes, were positioned in the geometric center of a dodecahedron-shaped container[32,33].

After conducting MDS, an analysis was performed on the trajectory to investigate several properties, such as root mean square fluctuation (RMSF), root mean square deviation (RMSD), and radius of gyration (Rg). The results were analysed using Maestro graphic user interface (GUI).

***In silico* pharmacokinetics**

Before commencing the investigational process, it is necessary to first investigate the absorption, distribution, metabolism, elimination, and toxicity (ADMET) of these substances within the human body. This is necessary to ensure that the new medication can be identified with a high rate of success while simultaneously shortening the amount of time required for the experimental research. In order to achieve this purpose, we investigated the pharmacokinetic *in silico* tools *i.e*., pkCSM for novel compounds that had been tested in the management of AD[34,35].

Results and Discussion

Establishment of a structure-based pharmacophore model

The concept of pharmacophore refers to the spatial configuration of crucial steric and electronic characteristics that facilitate the most favourable interaction between a ligand and a macromolecule. The selection of the pharmacophore model may vary depending on the information available, with the choice being either structure-based or ligand-based,

corresponding to the availability of target or known ligand data, respectively. The present study involved the construction of a structure-based pharmacophore model. This model was developed by identifying and incorporating the common features from two separate pharmacophore models[36]. These initial models were designed based on the X-ray structures of two enzymes, AChE and BuChE, which were bound to two highly effective inhibitors: donepezil and N-((1-benzylpiperidin-3-yl) methyl)-N-(2-methoxyethyl) naphthalene-2-sulfonamide. A pharmacophore model consisting of six characteristics was constructed using DS 2.0 software, as seen in the Fig. 1.

Validation of pharmacophore model

GH scoring was carried out using the database of 392 compounds (AChE) and 400 compounds (BuChE) which was taken from the literature. With AChE-based pharmacophore; 47 compounds were known as actives (A), 29 compounds as total hits (H_t), 25 compounds belong to known actives (H_a), and the value of false negative was observed to be 4. In the BuChE-based pharmacophore, 69 compounds were known as actives (A), 55 compounds as total hits (H_t), 48 compounds belonged to known actives (H_a), and the value of false negative was observed to be 7. GH scoring was observed to be 0.779 for AChE and 0.828 for BuChE, which is greater than the recommended GH scoring value (>0.5), indicating the profoundness of the model[26]. The results are presented in **Table S1**.

Screening of database

The validated pharmacophore was further used as a three-dimensional query for virtual screening of the ZINC database for retrieval of compounds with similar features and inter-atomic distances. The BEST search option available in DS was used to find hits[24]. In AChE and BuChE enzyme-based pharmacophores, the virtual screening results revealed that 100 hits are mapping on all pharmacophoric features and have complimentary inter-atomic distances. These compounds were also examined for Lipinski violation, and it was observed that 85 (AChE) and 86 (BuChE) compounds followed Lipinski's rule of five, remaining compounds were excluded as shown in **Fig. S1**. The remaining 85 (AChE) and 86 (BuChE) compounds were scrutinized based on their fit value and estimated value including higher than 6.5 and below 21 nM respectively. This aforementioned process retained 11 compounds as mentioned in Table 1 and Table 2.

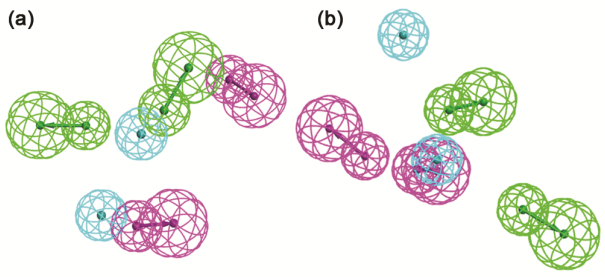

Fig. 1 — SBDD-based pharmacophore (a) AChE, (b) BuChE

Molecular docking studies

The retrieved 11 compounds **ZINC000408960314**, **ZINC000001693021**, **ZINC000257331938**, **ZINC000409352506**, **ZINC000409357823**, **ZINC000245204495**, **ZINC000329492445**, **ZINC000328889866**, **ZINC000013225671**, **ZINC000073353208** and **ZINC000102717880** were docked against AChE (4ey7) and BuChE (5dyw) macromolecules active binding sites and found that **ZINC000329492445**, **ZINC000001693021**, and **ZINC000257331938** compounds showed good binding score as presented in Table 3 and Fig. 2 and Fig. 3. In the active pockets of AChE, compound **ZINC000329492445** showed the binding affinity -98.546 Kcal/mol. It interacts with Ser203, Gly122, and Gly121 through conventional hydrogen bond and carbon-hydrogen bond, showed π-sulfur bond interaction with Phe338, π-π stacked bond interactions with Trp86 and π-alkyl bond interaction with Trp86 amino acid residues. Whereas, in the active site of BuChE, compound **ZINC000329492445** showed a binding affinity of -143.955 Kcal/mol and displayed various binding interactions including hydrogen bond interactions with Ser198, Gly117, Gly116, His438, and Thr120, π-sulfur bond interactions with Trp231, Phe329, and Phe398, and π-alkyl interaction with Trp82 and His438 amino acids residues.

The isopropyl amino group of the **ZINC000001693021** compound demonstrated hydrogen binding with His447 amino acid, various hydrophobic bindings *viz* π-alkyl bond and alkyl with Leu130, Trp86, Tyr341, Tyr337, Phe338, Phe295 and Phe297 amino acid residues of AChE with -107.213 Kcal/mol binding affinity, wherein compound **ZINC000001693021** showed hydrogen bond interaction with His438 and hydrophobic interactions with π-π T-shaped with Phe329, alkyl bond with Trp231 and π-alkyl bond with Val288 and Leu286 amino acid residues of the BuChE with -96.9115 Kcal/mol binding energy.

Table 1 — Structure-based pharmacophore model of AChE

Ache (4ey7)	Fit value	RMSD	Mapping	Features mapping
ZINC000408960314	1.30688	0.414	4	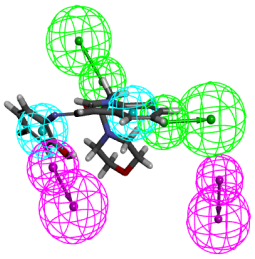
ZINC000001693021	2.22652	0.34	3	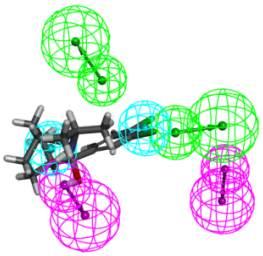
ZINC000257331938	1.226	0.375	4	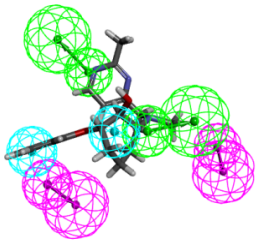
ZINC000409352506	0.15573	0.352	4	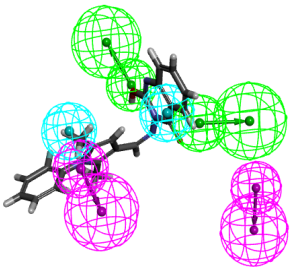
ZINC000409357823	0.168191	0.393	4	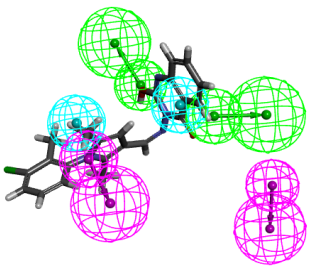
ZINC000245204495	2.70883	0.401	4	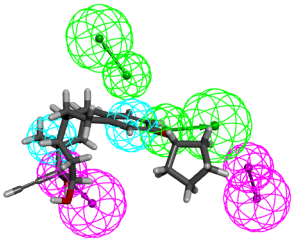

(*Contd.*)

Table 1 — Structure-based pharmacophore model of AChE (*Contd*.)

Ache (4ey7)	Fit value	RMSD	Mapping	Features mapping
329492445	2.41425	0.327	3	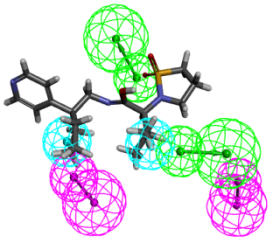
328889866	2.11571	0.396	3	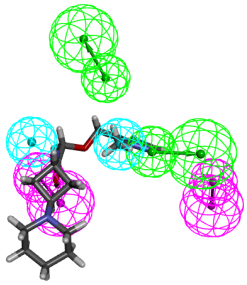
ZINC000013225671	0.404285	0.35	4	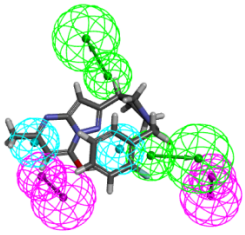
ZINC000073353208	1.43986	0.406	4	
ZINC000102717880	2.31981	0.384	3	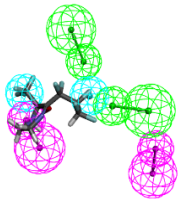

For **ZINC000257331938** compound, the nitrogen group of the pyrimidine ring and hydroxyl group of the cyclohexanol ring exhibited hydrogen bonds with His447, Gly122, and Gly121 amino acid residues, hydrophobic interactions including π-π T-shaped, π-sigma, π-π stacked, alkyl and π-alkyl bond interactions with Trp86, Tyr337, Trp236, Phe297 and Ala204 amino acid residues with -127.157 Kcal/mol binding affinity against AChE , wherein, pyrimidine ring and hydroxy group of cyclohexanol ring also involved in the formation of conventional hydrogen bonds with Glu197 and carbon-hydrogen bond with Gly121, Thr120, and Ser198 amino acid residues, π-π stacked bond with Trp82, alkyl and π-alkyl bonds Leu286, Tyr114, Tyr128 and Leu125 amino acid residues with -125.586 Kcal/mol binding affinity against BuChE.

In the docking studies, it was found that all the lead molecules were well accommodated in the pocket of the AChE and BuChE. Overall binding interactions of the lead molecules with both enzymes suggest that hydrophobic and hydrogen bond formation play a key role in stabilizing these ligands in the catalytic site. The crucial amino acids at the AChE cavity were

Table 2 — Structure-based pharmacophore model of BuChE

BuChE (5dwy)	Fit value	RMSD	Mapping	Feature mappings
ZINC000408960314	2.86348	0.414	3	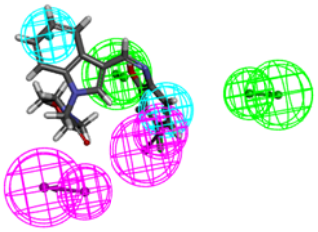
ZINC000073353208	2.52099	0.406	4	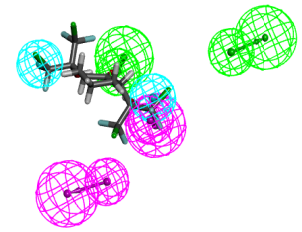
ZINC000257331938	2.69665	0.375	3	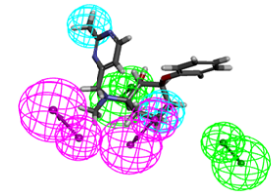
328889866	2.53936	0.396	3	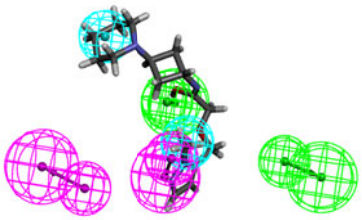
ZINC000102717880	2.50226	0.384	3	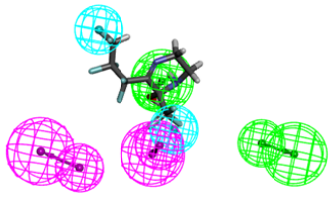
ZINC000013225671	2.53118	0.35	3	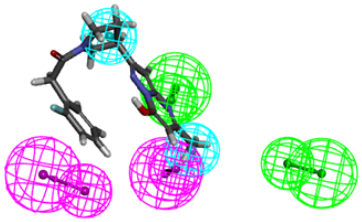
329492445	2.56062	0.327	4	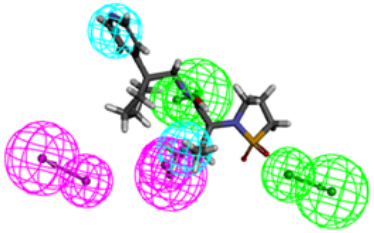

(*Contd.*)

Table 2 — Structure-based pharmacophore model of BuChE (*Contd*.)

BuChE (5dwy)	Fit value	RMSD	Mapping	Feature mappings
ZINC000245204495	2.59009	0.401	4	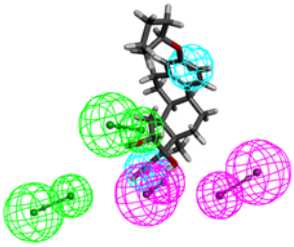
ZINC000409357823	2.67664	0.393	3	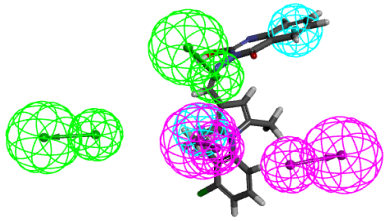
ZINC000001693021	2.70813	0.34	3	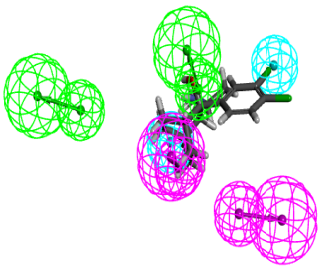
ZINC000409352506	2.68748	0.352	3	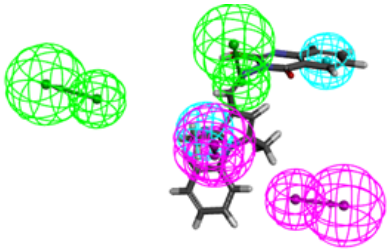

Table 3 — Binding energy and interactions of potent compounds at the active site AChE and BuChE

Compd	AChE (4ey7)		BuChE (5dyw)	
	Binding energy (Kcal/mol)	Amino acid residues with H-bond distance (Å)	Binding energy (Kcal/mol)	Amino acid residues with H-bond distance (Å)
ZINC000329492445	-98.546	O-Gly121 (2.339), O-Gly121 (2.105), O-Gly122 (1.902), O-Ser203 (2.671)	-143.955	O-Gly117 (2.314), O-Gly117 (2.847), O-Ser198 (2.490), N-Gly116 (2.819)
ZINC000001693021	-107.213	H-His447 (2.353)	-96.911	O-His438 (2.756)
ZINC000257331938	-127.157	N-Gly121 (2.803), N-Gly121(2.023), H-His447 (2.302)	-125.586	O-Ser198 (2.671), H-Glu197 (3098), H-Thr120 (2.741)

found to be Ser203, Phe295, Tyr72, Trp286, Tyr341, Tyr337, Phe338, and Trp86. Similarly, in the active binding cavity of BuChE, various amino acid residues crucial for binding with the ligands were found to be Thr120, Asn68, Gly116, Leu286, Trp231, Phe329, Tyr332, Ala328, and Trp82 as important amino acid residues.

Molecular dynamic simulation

MD simulation was performed using the Desmond package on the compounds with the most significant predicted binding energies above -80.00 Kcal/mol. Docked complexes **ZINC000329492445**, **ZINC000001693021**, and **ZINC000257331938**) were investigated for 100 ns MD simulations. Through the

analysis of the RMSD values between the initial end simulated trajectories, the basic properties and conformational features of the protein-ligand complexes were evaluated. The average RMSD of the enzyme 4ey7-ligand complex involving **ZINC000329492445**, **ZINC000001693021**, and **ZINC000257331938** were determined 1.32, 1.38, and 1.59 Å, respectively, as depicted in **Table S2**. Similarly, RMSD values for the 5dyw-ligand complex with **ZINC000329492445**, **ZINC000001693021**, and **ZINC000257331938** were found to be 2.48, 0.29, and 1.60 Å (**Table S3)**. RMSD values indicate the significant binding of ligands with the AChE and BuChE demonstrating their efficacy.

The calculation of binding energies and binding interactions involving the AChE and targeted ligands were carried out using MD simulations, illustrated in **Table S2** and Fig. 4, Fig. 5 and Fig. 6. **ZINC000329492445** compound exhibited hydrogen bond interactions with the Tyr124, Ser125, Glu202, Tyr337, and His447 with AChE enzyme, hydrophobic interactions with the Trp86, Glu202, Phe338, Tyr341, and Tyr449; water bridge with Gln71, Tyr72. Asp74, Asn87, Gly122, Gly126 amino acid residue of the AChE. The compound **ZINC000329492445** exhibited minimal structural changes throughout the range of 22.7 to 23.2 Å, indicating a rather stable alignment throughout the binding region (**Fig. S2**). In the similar manner, compound **ZINC000001693021** participated in the hydrogen bond interactions with Tyr124 and Tyr341; hydrophobic interactions with Tyr72, Leu76, Tyr77, Trp86, Val294, Phe295, Phe297, Tyr337, Phe338, Val340, Trp439 and water bridge interactions with Tyr124, Arg296 and Tyr341amino acid residues of AChE. The compound **ZINC000001693021** exhibited minimal structural alterations within the range of 22.7 to 23.3 Å, indicating a rather stable orientation inside the binding site (**Fig. S2**). Compound **ZINC000257331938** also exhibited hydrogen bond interaction with several amino acid residues including Gly121, Tyr124, Ser125, Glu202, Tyr341 and His447; hydrophobic interactions with Val73, Tyr77, Met85, Trp86, Ala127, Leu130, Phe297, Tyr337 and Phe338, and water bridge interactions with Tyr72, Asp74, Met85, Gly122,

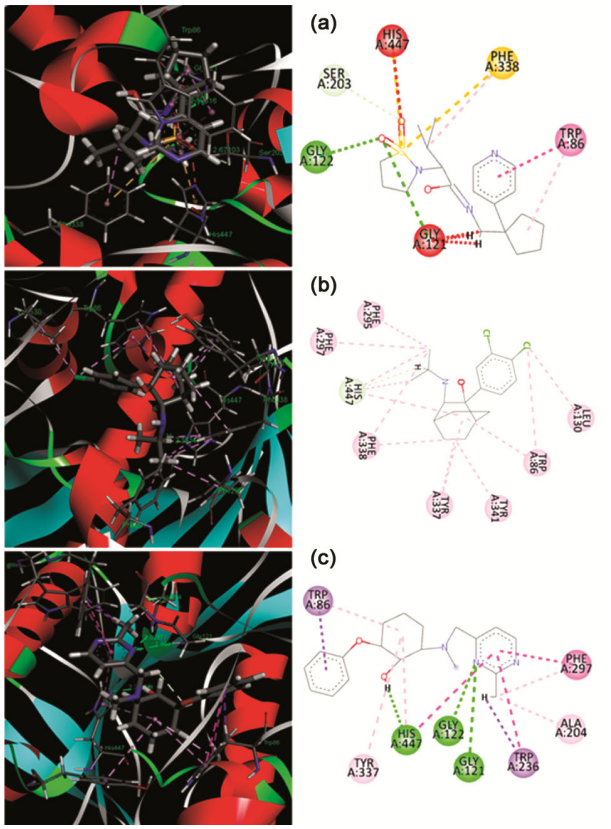

Fig. 2 — 2D and 3D binding interactions of **ZINC000329492445**, **ZINC000001693021**, and **ZINC000257331938** at the active site AChE (PDBID: 4ey7).

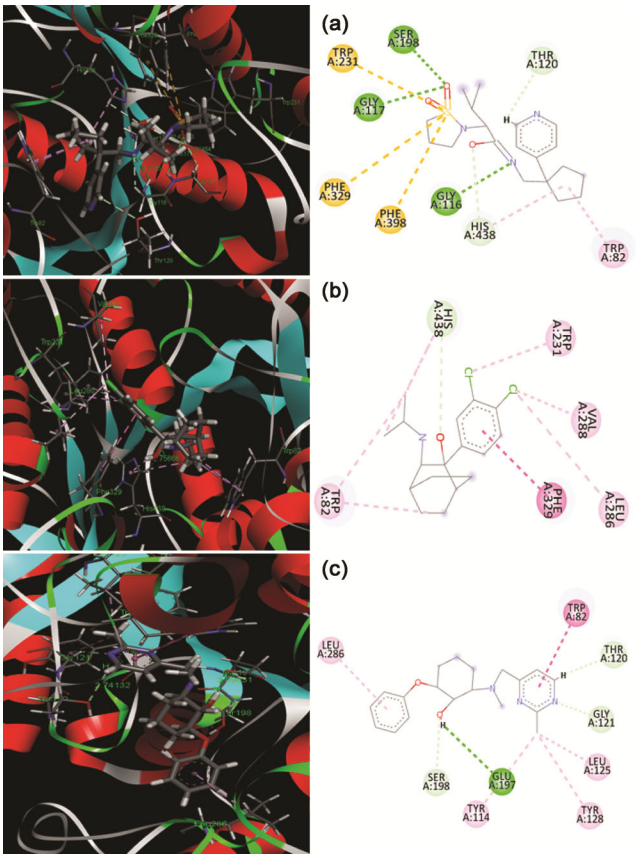

Fig. 3 — 2D and 3D binding interactions of **ZINC000329492445**, **ZINC000001693021**, and **ZINC000257331938** compounds with BuChE enzyme (5dyw).

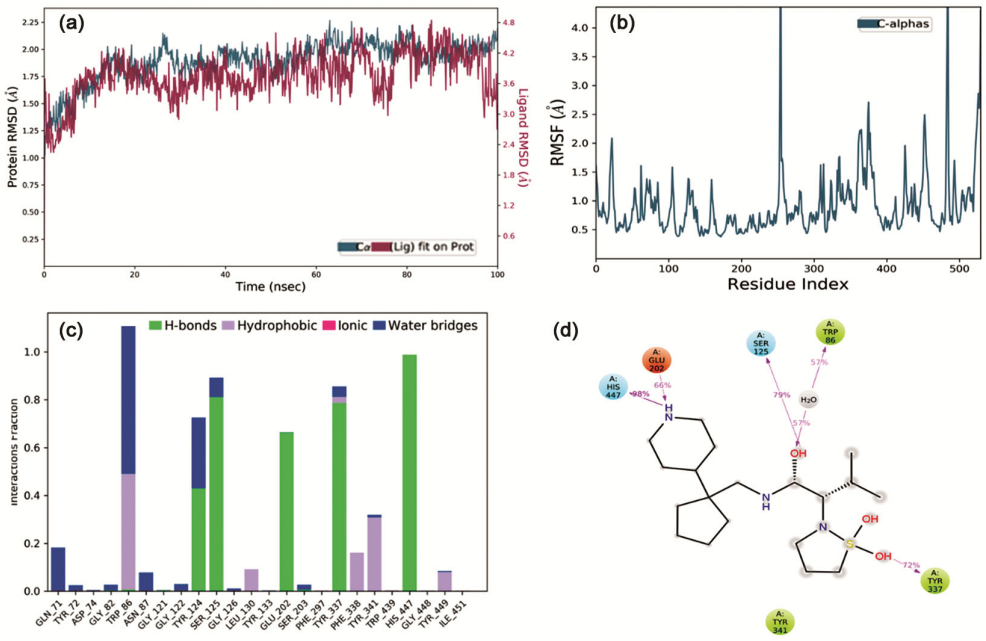

Fig. 4 — Molecular dynamic studies of complex **ZINC000329492445**-AChE for 100 ns: (a) RMSD analysis of **ZINC000329492445**; (b) RMSF analysis of **ZINC000329492445**; (c) Binding interactions analysis of **ZINC000329492445**; (d) Percentage protein-ligand interaction of **ZINC000329492445**.

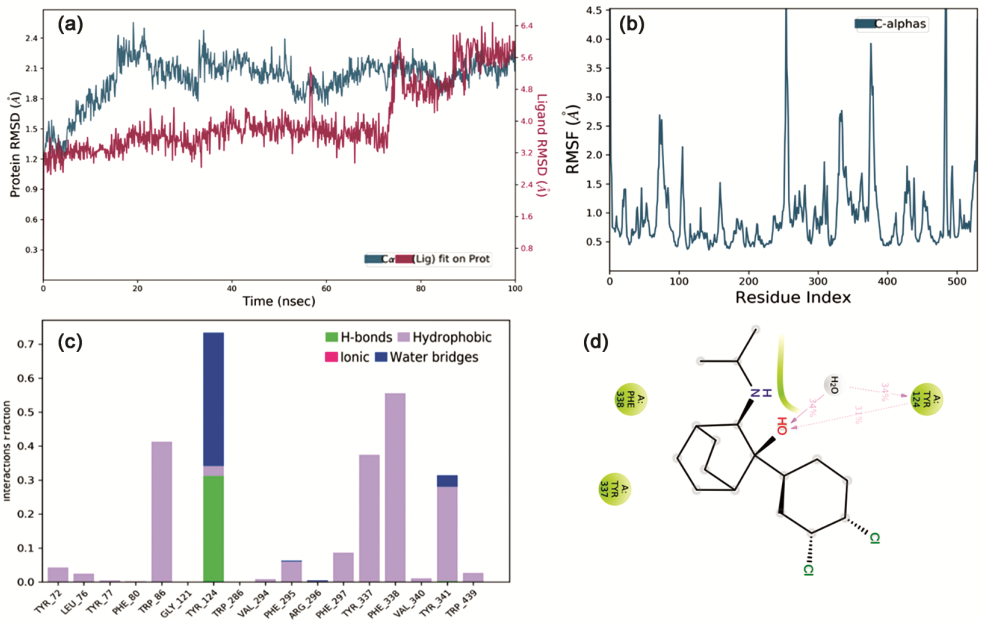

Fig. 5 — Molecular dynamic studies of complex **ZINC000001693021**-AChE for 100 ns: (a) RMSD analysis of **ZINC000001693021**; (b) RMSF analysis of **ZINC000001693021**; (c) Binding interactions analysis of **ZINC000001693021**; (d) Percentage protein-ligand interaction of **ZINC000001693021**.

Ser125, Ser203, Tyr341 and Gly342 amino acid residues of AChE. The compound **ZINC000257331938** exhibited a reduced number of structural changes throughout the range of 22.7 to 23.4 Å, indicating a rather stable orientation inside the binding site (**Fig. S2**).

Similarly, the binding energies, and binding interactions of BuChE docked complexes were evaluated using MD simulations and presented in **Table S3** and Fig. 7, Fig. 8 and Fig. 9. Compound **ZINC000329492445** demonstrated hydrogen bond interactions with several amino acid residues in the

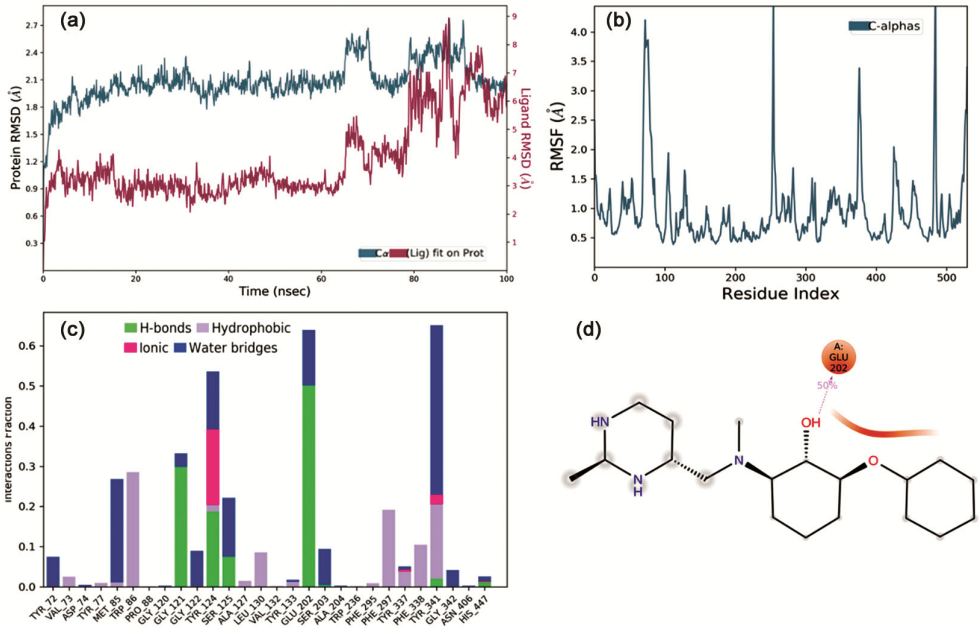

Fig. 6 — Molecular dynamic studies of complex **ZINC000257331938**-AChE for 100 ns. (a) RMSD analysis of **ZINC000257331938**; (b) RMSF analysis of **ZINC000257331938**; (c) Binding interactions analysis of **ZINC000257331938**; (d) Percentage protein-ligand interaction of **ZINC000257331938**.

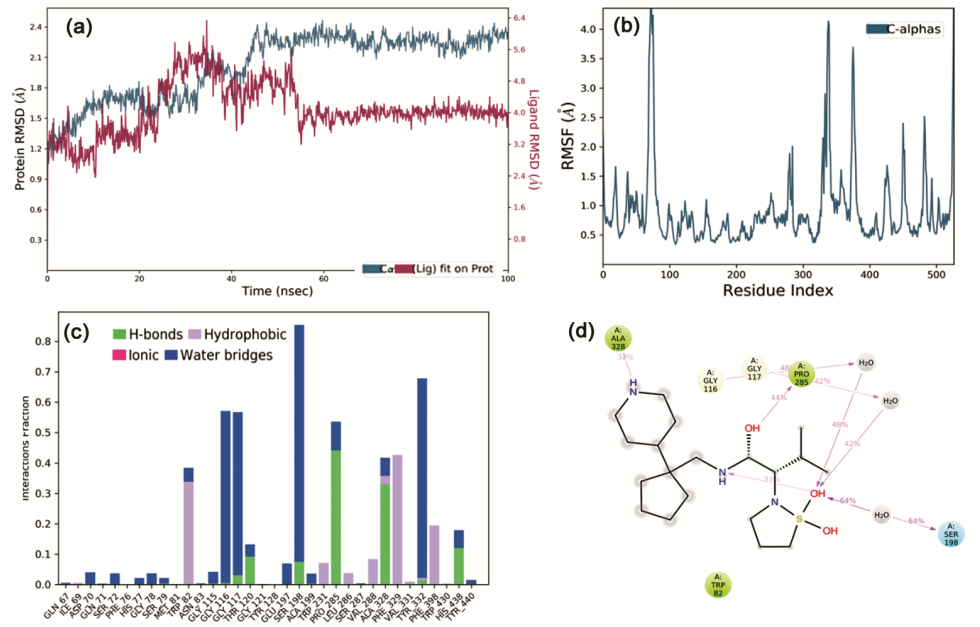

Fig. 7 — Molecular dynamic studies of complex **ZINC000329492445**-BuChE for 100 ns: (a) RMSD analysis of **ZINC000329492445**; (b) RMSF analysis of **ZINC000329492445**; (c) Binding interactions analysis of **ZINC000329492445**; (d) Percentage protein-ligand interaction of **ZINC000329492445**.

active site, including Gly116, Gly117, Thr120, Ser198, Pro285, Ala328, Tyr332, and His438. Additionally, it exhibited hydrophobic interactions with Trp82, Trp231, Leu286, Val288, Phe329, Val331, Phe398, and Trp430 amino acid residues. Furthermore, the compound formed water bridge interactions with Gln67, Asp70, Gln71, Ser72, His77, Gly78, Sr79, Gly115, Glu197, Ala199, and Tyr440 amino acid residues of the BuChE. The compound **ZINC000329492445** exhibited minimal structural changes throughout the range of 22.9 to 23.4 Å, indicating a rather stable orientation inside the binding

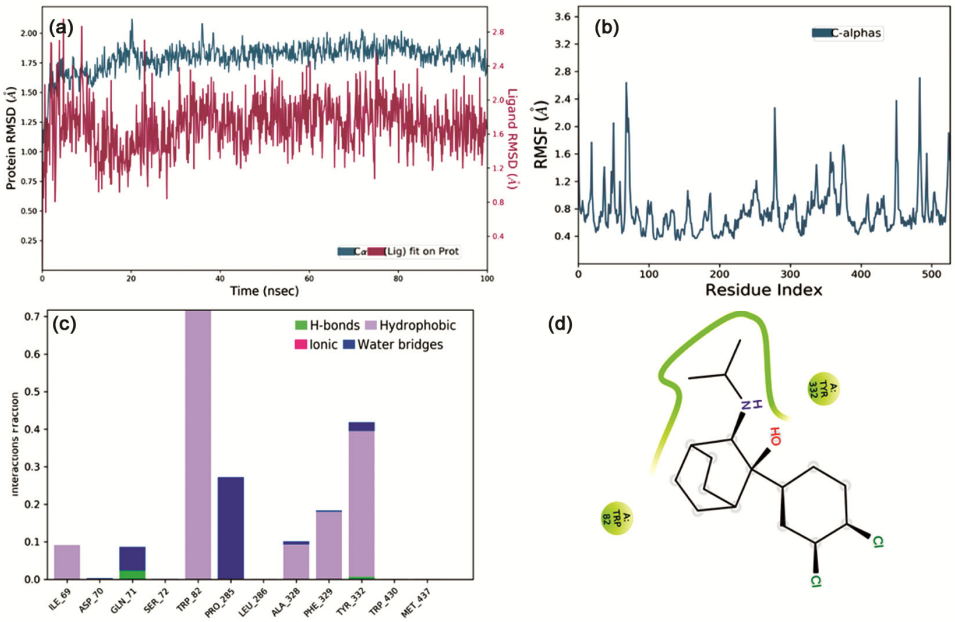

Fig. 8 — Molecular dynamic studies of complex **ZINC000001693021**-BuChE for 100 ns: (a) RMSD analysis of **ZINC000001693021**; (b) RMSF analysis of **ZINC000001693021**; (c) Binding interactions analysis of **ZINC000001693021**; (d) Percentage protein-ligand interaction **ZINC000001693021**.

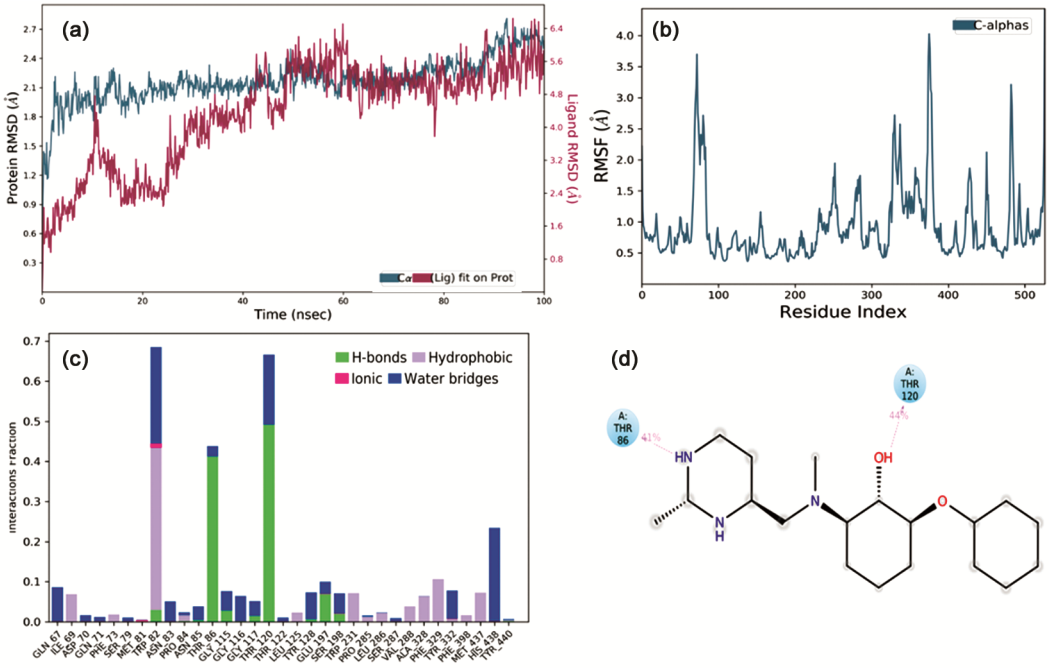

Fig. 9 — Molecular dynamic studies of complex **ZINC000257331938**-BuChE for 100 ns: (a) RMSD analysis of **ZINC000257331938**; (b) RMSF analysis of **ZINC000257331938**; (c) Binding interactions analysis of **ZINC000257331938**; (d) Percentage protein-ligand interaction **ZINC000257331938**.

site (**Fig. S2**). Compound **ZINC000001693021** exhibited hydrogen bond interactions with Gln71 and Tyr332, as well as hydrophobic contacts with Ile69, Trp82, Ala328, Phe329, and Tyr332. Additionally, it formed water bridge connections with Asp70, Pro285, Gln71, and Tyr332 amino acid residues of the BuChE enzyme. The compound **ZINC000001693021** exhibited minimal structural changes throughout the range of 22.9 to 23.3 Å, indicating a rather stable orientation inside the binding site (**Fig. S2**). Compound

ZINC000257331938 exhibited hydrogen bond interactions with Trp82, Asn85, Thr86, Gly115, Gly117, Thr120, Tyr128, Glu197, and Ser198 amino acid residues. Additionally, it engaged in hydrophobic interactions with Ile69, Phe73, Pro84, Leu125, Trp231, Val288, Ala328, Phe329, Phe398, and Met437 amino acid residues. Furthermore, the compound formed water bridge interactions with Gln67, Asp70, Gln71, Ser79, Asn83, Asn85, Thr120, Ser287, and His438 amino acid residues of the BuChE. The compound **ZINC000257331938** exhibited a reduced number of structural changes throughout the range of 22.9 to 23.4 Å, indicating a rather stable orientation inside the binding site (**Fig. S2**).

Drug-likeness, Physicochemical, and ADMET properties

Identified lead compounds were assessed drug-likeness, physicochemical, and ADMET properties as presented in Table 4. The compounds exhibited drug-likeness as per Lipinski rule; hydrogen bond acceptors (4, 2, and 5), hydrogen bond donors (1, 2, and 1), rotatable bonds (6, 3, 5) and molecular weight <500 (Ref. 37). Therefore, the obtained search results demonstrated satisfactory drug-like characteristics, suggesting their potential as therapeutic agents.

Furthermore, obtained leads were screened for ADME-related metrics, including molecular mass (MW), octanol-water partition coefficients (LogP), topological polar surface area (TPSA), water solubility, gastrointestinal absorption (GIA), and blood-brain barrier (BBB) permeability (Table 4). All screened compounds have been shown to exhibit insufficient absorption when their TPSA surpasses the established threshold of 140 $Å^2$, which acts as a benchmark for authorised drugs[18,38–40]. A significant correlation has been observed between the TPSA and the mass of molecules. The permeability properties of screened compounds against GIA and BBB showed significance in the realm of formulating a therapeutic intervention intended for widespread use. All three compounds that were obtained had adequate GIA and displayed the ability to effectively cross the BBB.

Table 4 — Drug-likeness, physicochemical and ADMET properties of lead compounds

Class	Properties	**ZINC000329492445**	**ZINC000001693021**	**ZINC000257331938**
Physicochemical properties	Mol. Wt. (g/mol)	379.53	328.28	327.43
	Lipophilicity(clogP)	1.22	4.11	1.8
	Solubility	-3.42	-5.03	-2.01
	TPSA ($Å^{2)}$	91.24	32.26	58.48
	Drug likeness	-2.18	2.22	1.53
	Drug Score	0.45	0.57	0
	H bond acceptor	4	2	5
	H bond donor	1	2	1
	Rotatable bond	6	3	3
	Violation	0	0	0
	Bioavailability score	0.55	0.55	0.55
Absorption	GI Absorption	High	High	High
Metabolism	CYP2D6 substrate	No	No	Yes
	CYP3A4 substrate	No	No	No
	CYP1A2 inhibitor	No	No	No
	CYP2C19 inhibitor	No	Yes	No
	CYP2C9 inhibitor	No	No	No
	CYP2D6 inhibitor	No	No	yes
	CYP3A4 inhibitor	No	No	No
Distribution	BBB	High	High	High
	Plasma Protein Binding (PPB)	Yes	Yes	Yes
Excretion	Total clearance (log mL/min/kg)	1.419	0.937	0.726
Toxicity	AMES mutagenicity	No	No	No
	Oral Rat Acute Toxicity (LD50) (mol/kg)	2.062	2.362	2.321
	Hepatotoxicity	Yes	Yes	No
	Skin Sensitisation	No	No	No
	Carcinogenicity	No	No	No

Cytochrome P450s (CYPs) are a substantial group of enzymes that include heme and play a crucial role in the process of eliminating foreign substances and metabolizing pharmaceutical compounds. The activity of cytochrome P450 enzymes may be modulated by pharmaceutical agents, leading to noteworthy drug-drug interactions with potential implications for clinical practice. These interactions may give rise to unexpected side effects or therapeutic inefficacy[41]. All three substances were anticipated to function as a substrate for the enzyme CYP3A4. The compounds **ZINC000329492445** and **ZINC000001693021** exhibited inhibition when exposed to the CYP2C19 enzyme. Additionally, **ZINC000001693021** showed inhibition when subjected to the CYP2D6 and CYP3A4 enzymes. Furthermore, both compounds exhibited a poor clearance rate.

The assessment of toxicity included the examination of acute oral toxicity, AMES mutagenesis, carcinogenicity, and hepatotoxicity were also determined (Table 4). There were no observed instances of AMES mutagenesis or carcinogenicity among any of the compounds. However, it was expected that **ZINC000329492445** and **ZINC000257331938** exhibited hepatotoxicity towards hepatocytes.

Conclusion

In present work, we have developed and validate the pharmacophore models for both AChE and BuChE. The optimal pharmacophore models comprise of two HBA, two HBD, and two HY. The models were used to identify 11 compounds through molecular docking studies, to enumerate the key interactions in the active site of AChE and BuChE. The identified lead compounds **ZINC000329492445**, **ZINC000001693021**, and **ZINC000257331938**, exhibited a consistent interaction mechanism with Ser203, Trp86, and Phe338 in the binding site of hAChE, as well as with Gly117, His448, and Ser198 in the binding site of hBuChE. Furthermore, **ZINC000329492445**, **ZINC000001693021**, and **ZINC000257331938** were subjected for molecular dynamics studies. The data revealed compounds show the significant compliance with docking studies for the simulation period of 100 ns. Moreover, the lead compounds showed accepted drug-likeness and ADME properties. Therefore, the compounds **ZINC000329492445**, **ZINC000001693021**, and **ZINC000257331938**, identified using computational methods, have the potential to develop as dual inhibitors targeting both human acetylcholinesterase and butyrylcholinesterase.

Supplementary Information

Supplementary information is available in the website http://nopr.niscpr.res.in/handle/123456789/58776.

Conflict of interest

All authors declare no conflict of interests.

Acknowledgement

Poonam Yadav is thankful to the GLA University for providing the necessary facility to conduct the research.

Funding

No funding is associated with this work.

Author contributions

Dr Shivani Jaiswal contributed to conceptualization, supervision, writing-review and editing; Poonam Yadav contributed to investigation, formal analysis, draft writing.

References

1 Sajid M I, Sheikh F S, Anis F, Nasim N, Sumbria R K, Nauli S M & Tiwari R K, *Adv Drug Deliv Rev,* 199 (2023) 114968.
2 Si Z Z, Zou C J, Mei X, Li X F, Luo H, Shen Y, Hu J, Li X X, Wu L & Liu Y, *Neural Reg Res,* 18 (2023) 708.
3 Athar T, Balushi K A & Khan S A, *Mol Biol Rep*, 48 (2021) 5629.
4 Kumar S, *Indian J Pharm*, , 47 (2015) 444.
5 Thompson K J & Tobin A B, *Signal Cell*, 70 (2020) 109545.
6 Silva V B D, Andrade P D, Kawano D F, Morais P A B, Almeida J R D, Carvalho I, Taft C A & Silva C H T D P D, *Fut Med Chem,* 3 (2011) 947.
7 Chen Y, Lin H, Yang H, Tan R, Bian Y, Fu T, Li W, Wu L, Pei Y & Sun H, *RSC Adv,* 7 (2017) 3429.
8 Masters C L, Bateman R, Blennow K, Rowe C C, Sperling R A & Cummings J L, *Nat Rev Dis Prim*, 11 (2015) 1.
9 Hampel H, Mesulam M M, Cuello A C, Farlow M R, Giacobini E, Grossberg G T, Khachaturian A S, Vergallo A, Cavedo E, Snyder P J & Khachaturian Z S, *Brain*, 141 (2018) 1917.
10 Acosta M F, Muralidharan P, Grijalva C L, Abrahamson M D, Hayes D, Fineman J R, Black S M & Mansour H M, *Ther Adv Res Dis*, 15 (2021) 1.
11 Li S Y, Jiang N, Xie S S, Wang K D G, Wang X B & Kong L Y, *Org Biomol Chem*, 12 (2014) 801.
12 Oboh G, Adedayo B C, Adetola M B, Oyeleye I S & Ogunsuyi O B, *Drug Chem Toxicol*, 45 (2022) 731.
13 Gupta M, Ojha M, Yadav D, Pant S & Yadav R, *ACS Chem Neurosci*, 11 (2020) 2849.
14 Zhou S, Yuan Y, Zheng F & Zhan C G, *Chem Biol Interact*, 308 (2019) 372.
15 Assis P M D, Fávero A, Menegasso J F, Meinel R S, Marion G M, Nunes V S P, Goliatt P V Z C, Silva A D da, Dutra R C & Raposo N R B, *Life Sci* , 249 (2020) 117538.
16 Dhanjal J K, Sharma S, Grover A & Das A, *Biomed Pharmacoth*, 71 (2015) 146.

17 Irwin J J, Tang K G, Young J, Dandarchuluun C, Wong B R, Khurelbaatar M, Moroz Y S, Mayfield J & Sayle R A, *J Chem Inf Model*, 60 (2020) 6065.
18 Pal S, Kumar V, Kundu B, Bhattacharya D & Preethy N, *Comp Struc Biotech J,* 17 (2019) 291.
19 Cheung J, Rudolph M J, Burshteyn F, Cassidy M S, Gary E N, Love J, Franklin M C & Height J J, *J Med Chem*, 55 (2012) 10282.
20 Košak U, Brus B, Knez D, Šink R, Žakelj S, Trontelj J, Pišlar A, Šlenc J, Gobec M, Živin M, Tratnjek L, Perše M, Sałat K, Podkowa A, Filipek B, Nachon F, Brazzolotto X, Więckowska A, Malawska B, Stojan J, Raščan I M, Kos J, Coquelle N, Colletier J P & Gobec S, *Sci Rep*, 6 (2016) 39495.
21 Giordano D, Biancaniello C, Argenio M A & Facchiano A, *Pharmaceuticals*, 15 (2022) 646.
22 Maia E H B, Assis L C, Oliveira T A D, Silva A M D & Taranto A G, *Front Chem*, 8 (2020) 481382.
23 Mishra P, Kesar S, Paliwal S K, Chauhan M & Madan K, *Cent Nerv Syst Agents Med Chem*, 18 (2018) 150.
24 Kumbhar N, Nimal S, Barale S, Kamble S, Bavi R, Sonawane K & Gacche R, *Sci Rep*, 12 (2022) 1.
25 Schepetkin I A, Nurmaganbetov Z S, Fazylov S D, Nurkenov O A, Khlebnikov A I, Seilkhanov T M, Kishkentaeva A S, Shults E E & Quinn M T, *Molecules*, 28 (2023) 3357.
26 Jang C, Yadav D K, Subedi L, Venkatesan R, Venkanna A, Afzal S, Lee E, Yoo J, Ji E, Kim S Y & Kim M H, *Sci Rep*, 8 (2018) 14921.
27 Zhou Y, Lu X, Yang H, Chen Y, Wang F, Li J, Tang Z, Cheng X, Yang Y, Xu L & Xia Q, *Mol*, 24 (2019) 4217.
28 Sharma M, Mittal A, Singh A, Jainarayanan A K, Sharma S & Paliwal S, *Biol Methods Protoc*, 5 (2021) 1.
29 Ashour M L, Youssef F S, Gad H A & Wink M, *Pharm Mag*, 13 (2017) 300.
30 Choubey P K, Tripathi A, Sharma P & Shrivastava S K, *Bioorg Med Chem*, 28 (2020) 115721.
31 Choubey P K, Tripathi A, Tripathi M K, Seth A & Shrivastava S K, *Bioorg Chem*, 111 (2021) 104922.
32 Gurung A B, Ali M A, Lee J, Farah M A & Al-Anazi K M, *Biomed Res Int*, 2021 (https://doi.org/10.1155/2021/8853056).
33 Arya H, Syed S B, Singh S S, Ampasala D R & Coumar M S, *Interdis Sci Comp Life Sci*, 10 (2018) 792.
34 Kollipara S, Ahmed T, Bhattiprolu A K & Chachad S, *Biopharm Drug Dispos*, 42 (2021) 297.
35 Pires D E V, Blundell T L & Ascher D B, *J Med Chem*, 58 (2015) 4066.
36 Mortier J, Dhakal P & Volkamer A, *Mol*, 23 (2018) 1959.
37 Shady N H, Mostafa N M, Fayez S, Abdel-Rahman I M, Maher S A, Zayed A, Saber E A, Khowdiary M M, Elrehany M A, Alzubaidi M A, Altemani F H, Shawky A M & Abdelmohsen U R, *Antioxidants*, 11 (2022) 1743.
38 Dwivedi N, Mishra B N & Katoch V M, *Bioinfo*, 7 (2011) 82.
39 Daina A, Michielin O & Zoete V, *J Chem Inf Mod*, 54 (2014) 3284.
40 Watanabe R, Esaki T, Kawashima H, Natsume-Kitatani Y, Nagao C, Ohashi R & Mizuguchi K, *Mol Pharm*, 15 (2018) 5302.
41 Shi Z, He Z & Wang D W, *Mol*, 27 (2022) 3873.